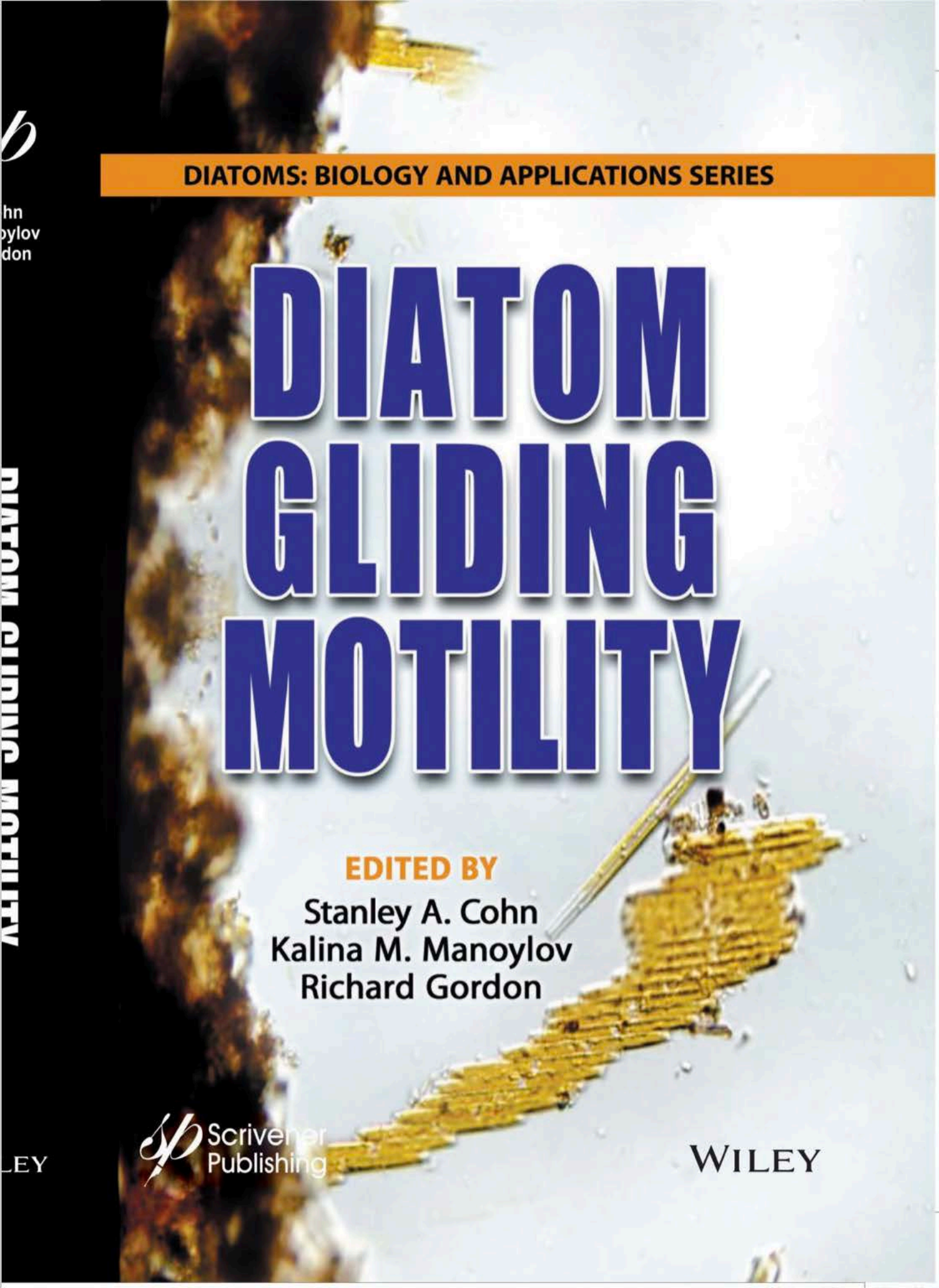
DIATOMS: BIOLOGY AND APPLICATIONS SERIES
DIATOM GLIDING MOTILITY
EDITED BY
Stanley A. Cohn
Kalina M. Manoylov
Richard Gordon
Scrivener Publishing
WILEY

Diatom Gliding Motility

Scrivener Publishing
100 Cummings Center, Suite 541J
Beverly, MA 01915-6106

Diatoms: Biology and Applications

Series Editors: Richard Gordon (dickgordoncan@xplornet.ca) and Joseph Seckbach (Joseph.Seckbach@mail.huji.ac.il)

Scope: The diatoms are a single-cell algal group, with each cell surrounded by a silica shell. The shells have beautiful attractive shapes with multiscalar structure at 8 orders of magnitude, and have several uses. 20% of the oxygen we breathe is produced by diatom photosynthesis, and they feed most of the aquatic food chain in freshwaters and the oceans. Diatoms serve as sources of biofuel and electrical solar energy production and are impacting on nanotechnology and photonics. They are important ecological and paleoclimate indicators. Some of them are extremophiles, living at high temperatures or in ice, at extremes of pH, at high or low light levels, and surviving desiccation. There are about 100,000 species and as many papers written about them since their discovery over three hundred years ago. The literature on diatoms is currently doubling every ten years, with 50,000 papers during the last decade (2006-2016). In this context, it is timely to review the progress to date, highlight cutting-edge discoveries, and discuss exciting future perspectives. To fulfill this objective, this new Diatom Series is being launched under the leadership of two experts in diatoms and related disciplines. The aim is to provide a comprehensive and reliable source of information on diatom biology and applications and enhance interdisciplinary collaborations required to advance knowledge and applications of diatoms.

Publishers at Scrivener
Martin Scrivener (martin@scrivenerpublishing.com)
Phillip Carmical (pcarmical@scrivenerpublishing.com)

Diatom Gliding Motility

Edited by

Stanley Cohn,

DePaul University, Chicago, IL, USA

Kalina Manoylov

Georgia College & State University, Milledgeville, GA, USA

and

Richard Gordon

Gulf Specimen Marine Laboratory & Aquarium, Panacea, FL, USA and Wayne State University, Detroit, MI, USA

WILEY

This edition first published 2021 by John Wiley & Sons, Inc., 111 River Street, Hoboken, NJ 07030, USA and Scrivener Publishing LLC, 100 Cummings Center, Suite 541J, Beverly, MA 01915, USA

For more information about Scrivener publications please visit www.scrivenerpublishing.com.

Wiley Global Headquarters
111 River Street, Hoboken, NJ 07030, USA

For details of our global editorial offices, customer services, and more information about Wiley products visit us at www.wiley.com.

Library of Congress Cataloging-in-Publication Data

ISBN 9781119526353

Cover image: Thomas Harbich
Cover design by Russell Richardson

Set in size of 11pt and Minion Pro by Manila Typesetting Company, Makati, Philippines

Printed in the USA

10 9 8 7 6 5 4 3 2 1

Contents

11

Diatom Triboacoustics

Ille C. Gebeshuber[1]*, Florian Zischka[1], Helmut Kratochvil[2], Anton Noll[3], Richard Gordon[4,5] and Thomas Harbich[6]

[1]Institute of Applied Physics, Vienna University of Technology, Vienna, Austria, Europe
[2]Department of Integrative Zoology, University of Vienna, Austria, Europe
[3]Austrian Academy of Sciences, Acoustics Research Institute, Vienna, Austria
[4]Gulf Specimen Marine Laboratory and Aquarium, Panacea, Florida, USA
[5]C.S. Mott Center for Human Growth and Development, Department of Obstetrics and Gynecology, Wayne State University, Detroit, Michigan, USA
[6]Independent Researcher, Am Brüdenrain, Weissach im Tal, Germany

Abstract

The aim of this work was to develop a method to record low-level sounds underwater in order to listen to possible sounds related to the gliding movement of raphid, motile diatoms, inspired by their jerky, high acceleration movements. Different techniques concerning the gathering and handling of diatoms and the possibilities of recording sounds related to their movement are presented.

A model was created to get a rough estimation of the expansion speed of mucopolysaccharide filaments. In a series of initial experiments, a hydrophone was used to get an idea of the acoustic situation. Furthermore some attempts to increase the density of raphid diatoms in a given volume were made. Though with these rough measurements no sounds could be detected, alternatives and advice on how to improve the experiment for future research are provided.

***Keywords*:** Diatom, pennate, benthic, locomotion, tribology, acoustics, hydrophone, snail

Glossary

accretion	Accumulation of material.
bulk modulus *K*	Describes the change of pressure that is necessary to cause a change of volume of a body.

**Corresponding author*: gebeshuber@iap.tuwien.ac.at
Ille C. Gebeshuber: gebeshuber@iap.tuwien.ac.at, https://orcid.org/0000-0001-8879-2302, http://www.ille.com
Florian Zischka: florian.zischka@aon.at, https://www.researchgate.net/profile/Florian_Zischka2
Helmut Kratochvil: helmut.kratochvil@univie.ac.at, https://www.nature.com/articles/srep44526, https://zoology.univie.ac.at/people/staff/helmut-kratochvil/, https://hekratochvil.hpage.com/wissenschaftliches.html
Anton Noll: anton.noll@oeaw.ac.at, https://www.researchgate.net/profile/Anton_Noll
Richard Gordon: dickgordoncan@xplornet.com
Thomas Harbich: thomas.harbich@diatoms.de, https://www.researchgate.net/profile/Thomas_Harbich, https://diatoms.de/en/

Stanley Cohn, Kalina Manoylov and Richard Gordon (eds.) Diatom Gliding Motility, (249–282)

chemotaxis Movement or orientation of organisms caused by chemical stimulus.

diatom Single-celled alga that forms an outer shell out of hydrated silicon dioxide.

ephemeral Volatile, vanishing quickly.

epipelic Residing at the interface of water and sediments (mud, clays and silt).

helictoglossa Internal, distal termination of the raphe.

hydrophone The underwater equivalent of a microphone. Used for recording sounds underwater.

inertial force Resistance of an object to change in its velocity.

millidyne A unit of force. 1 mdyne = 10^{-8} N

mucopolysaccharide Acid polysaccharide that protrudes from the raphe in the form of mucus filaments. They attach to the substratum and flow along the raphe. Through that the motive force for diatom locomotion could be generated.

pennate Regarding diatoms, species that form usually bilaterally symmetric shells typically elongated parallel to the raphes. Many pennate diatoms can use the raphe to move along a solid substrate though there are also pennate diatoms without a raphe (araphid).

photophobia When organisms react strongly to changes in light intensity, avoiding light.

phototaxis Movement or orientation of organisms caused by light stimulus.

plasmalemma Cell membrane that separates the interior of a cell from the outside environment.

protoplast Plant cell composed of nucleus, cytoplasm and plastids without a cell wall.

raphe A slit in the shell of diatoms which is connected to diatom motility.

raphe-sternum Thickened silica typically located along the apical axis of diatoms. Contains the raphe.

Reynolds number The Reynolds number is used for flow patterns in different fluid flow situations. At a low Reynolds number the flow is dominated by laminar flow, at a high Reynolds number turbulence occurs. The Reynolds number is the ratio of inertial force to viscous force:

$$Re = \frac{inertial\ force}{viscous\ force} = \frac{v \rho l}{\eta}$$

sound pressure The variations of pressure of a medium that occur due to propagation of sound waves through that medium, because sound waves are pressure waves.

triboacoustics The phenomenon of noise generated by friction, lubrication and wear.

vibrometer A measuring instrument for quantifying mechanical oscillation. Interference of laser light is used to measure the frequency and amplitude of an oscillation.

viscous force Resistive force on an object inside of a fluid due to the friction between the layers of the fluid.

11.1 State-of-the-Art

11.1.1 Diatoms and Their Movement

Diatoms are single-celled algae with an outer shell made from hydrated silicon dioxide. There are up to 200,000 different species in all kinds of forms and shapes. Raphid, motile diatoms - as the name suggests - have slits called raphes in their shells [11.28]:

> "*The raphe, as an organelle for the motion of the cells is commonly found in many pennate diatoms, but it occurs in very different structures. [...] Basically the raphe is a gap-shaped breach of the cell wall of more or less complexity.*" ([11.28], translated from German)

The raphe allows the diatoms to stick to surfaces and move along them. Previous work of Harper and Harper [11.26], where the adhesive forces of diatoms sticking on substrates as well as the tractive forces in the direction of motion were measured, showed that there is clearly a close relation between locomotion and adhesion. "In a total of over 500 observations, whenever a diatom moved it was adhering to the substrate." The amount of force is heavily dependent on the species considered and can reach from few to several hundreds of millidynes. "However, strong adhesion does not prevent movement: *Amphora ovalis* (Kützing, 1844) cells were able to move normally while exerting adhesions of over 400 millidynes" [11.26]. "There are also diatoms that do not separate after asexual reproduction, but adhere together and form chain-like colonies" [11.25]: *Bacillaria paxillifer* (O.F. Müller) Hendy (1951) even forms motile chains that can move around through water [11.1].

Sizes of diatoms range from 4–5 µm to up to 500 µm. "The highest speeds of locomotion occur in tidewater-diatoms. The maximum speed of *Navicula radiosa* (Kützing, 1844) amounts to 20 µm/s. *Pinnularia nobilis* (Ehrenberg, 1843) was able to cover a distance of 14 mm in 20 min, which equals almost 12 µm/s." ([11.28], translated from German).

The gliding movement of raphid, motile diatoms started to be the subject of research over 200 years ago [11.42] and over time various theories that tried to explain the mechanism were developed [11.22]. "According to some, the raphe is occupied by streaming cytoplasm, others proposed small flagella that protrude through the raphe slits" [11.36].

"Recent ideas have in common that the movement of the cell relative to the sub-stratum is considered to be mediated by the secretion of material from the raphe" [11.36]. In a model by Gordon, it is proposed that the hydration of mucopolysaccharide, the material the raphe is filled with and which is left behind as a mucilage trail, would provide sufficient motive force to explain the gliding motility of raphid diatoms [11.24] [11.21]. "Diatom movement appears to be smooth over short periods of time between reversals or stopping, but is in fact jerky, sudden accelerations and decelerations alternating with periods when the diatom is stationary or moving with constant velocity" [11.36].

Edgar [11.15] analyzed the speed and acceleration of several species of epipelic river diatoms using data from motion picture films of moving cells, examined frame-by-frame, and showed that large changes of speed occur within one tenth of a second, which is to be expected at that scale, because of the small inertial forces. Therefore, high speed cinematography is necessary to study the movements [11.15]. However, even at 890 frames per second, large accelerations between frames still occurred, pushing the limits of ordinary light microscopy [11.37]. Therefore, new approaches are needed to reach an understanding of what causes these huge, short-term accelerations, which is why we turned to triboacoustics.

Considerations of the jerky movement of a diatom in a highly viscous situation were made by Edgar [11.16]. Therefore, the effect of external forces on a moving diatom were discussed. The Reynolds number (*Re*) is the expression of the ratio of inertial force to viscous force.

$$Re = \frac{inertial\ force}{viscous\ force} = \frac{v\rho l}{\eta} \tag{11.1}$$

where: v = velocity, ρ = density of the fluid, l = size of body, η = viscosity of the fluid [11.16].

11.1.2 The Navier-Stokes Equation

The Navier-Stokes equation is the general equation of motion for the volume element dV of a viscous, flowing fluid. It results from Newton's second law, the basic equation of motion in classical mechanics: $\boldsymbol{F} = m \cdot \boldsymbol{a}$

The equation of motion for one mass element $\Delta m = \varrho \cdot \Delta V$ of a flowing medium is:

$$\boldsymbol{F} = \boldsymbol{F}_p + \boldsymbol{F}_g + \boldsymbol{F}_R = \Delta m \ddot{\boldsymbol{r}} = \rho \cdot \Delta V \cdot \frac{d\boldsymbol{u}}{dt} \tag{11.2}$$

where $u = \frac{dr}{dt}$ is the velocity of flow of the volume element dV [11.7].

With the terms:

$d\boldsymbol{F}_R = \eta \Delta \boldsymbol{u} dV$ (force of friction)
$d\boldsymbol{F}_p = -\boldsymbol{grad}(p) \cdot dV$ (force of pressure)
$d\boldsymbol{F}_g = \rho \boldsymbol{g} dV$ (gravity)

of the single forces and the acceleration:

$$\frac{d\boldsymbol{u}}{dt} = \frac{\partial \boldsymbol{u}}{\partial t} + (\boldsymbol{u} \cdot \nabla)\boldsymbol{u} \tag{11.3}$$

the equation of motion becomes the Navier-Stokes equation:

$$\rho\left(\frac{\partial}{\partial t} + \boldsymbol{u} \cdot \nabla\right)\boldsymbol{u} = -\boldsymbol{grad}\ p + p \cdot \boldsymbol{g} + \eta \Delta \boldsymbol{u} \tag{11.4}$$

For ideal liquids ($\eta = 0$) it becomes the Euler equation. The friction term $\eta \Delta \boldsymbol{u}$ turns the Euler equation (differential equation of first order) into an equation of second

order and thereby complicates solving it. On the right side of the Navier-Stokes equation there are the forces and on the left side the movement caused by those forces [11.7].

All dimensions of length can be scaled to one standard length l, all times to one standard time T and then all velocities $\boldsymbol{u}$ can be expressed as functions of l/T:

$$t = t' \cdot T \qquad \boldsymbol{u} = \boldsymbol{u}' \cdot \frac{l}{T}$$

$$\nabla = \frac{\nabla'}{L} \qquad p = p' \cdot \left(\frac{l}{T}\right)^2 \cdot \rho$$

where t', $\boldsymbol{u}'$, $\nabla' = l \cdot \left(\frac{\partial}{\partial x}, \frac{\partial}{\partial y}, \frac{\partial}{\partial z}\right)$ and p' are nondimensional quantities.

Through that, the Navier-Stokes equation (without the gravity term) becomes:

$$\frac{\partial \boldsymbol{u}'}{\partial t'} + (\boldsymbol{u}' \cdot \nabla')\boldsymbol{u}' = -\nabla' p' + \frac{1}{Re}\Delta' \boldsymbol{u}' \tag{11.5}$$

with the nondimensional Reynolds number:

$$Re = \frac{\rho \cdot l^2}{\eta \cdot T} = \frac{\rho \cdot v \cdot l}{\eta} \tag{11.6}$$

v = l/T has the dimension of a velocity. It defines the velocity of flow averaged over the length l. In ideal liquids $\eta = 0$ and therefore $Re = \infty$. In fluid dynamics that means that for viscous liquids with $\eta = 0$, currents are only similar when they take place in vessels with similar ratio of dimension and when they have the same Reynolds number Re. [11.7].

11.1.3 Low Reynolds Number

The following words from the wonderful publication *Life at Low Reynolds Number* by E.M. Purcell [11.33] lead to a better understanding of the meaning of situations at very low Reynolds number:

> "The Reynolds number for a man swimming in water might be 10^4. For a goldfish it might get down to 10^2. At very low Reynolds number of about 10^{-4} or 10^{-5} inertia is totally irrelevant. [...] As an example an animal of about a micron (= 1 μm) in size may move through water, where the kinematic viscosity is 10^{-2} cm/s, at a typical speed of 30 m/s. If the driving force for the movement of that animal suddenly ceases, it will only coast for about 0.1 Å and it takes about 0.6 s to slow down. This makes clear what low Reynolds number means. Inertia plays no role whatsoever. If you are at very low Reynolds number, what you are doing at the moment is entirely determined by the forces that are exerted on you at that moment, and by nothing in the past" [11.33].

Also, according to Purcell [11.33], at low Reynolds number a living being can't shake off its environment. "If it moves, it takes it along; it only gradually falls behind. [...] In that context diffusion is very important, because at low Reynolds number stirring isn't very good." Purcell also showed that the transport of wastes away from the animal and food to the animal is entirely controlled locally by diffusion: "It can thrash around a lot, but the fellow who just sits there quietly waiting for stuff to diffuse will collect just as much."

Also, an increased velocity of the moving animal is not beneficial for gaining more nutrients: "*To increase its food supply by 10% it would have to move at a speed of 700 μm/sec, which is 20 times as fast as it can swim. The increased intake varies like the square root of the bug's velocity so the swimming does no good at all in that respect. But what it can do is find places where the food is better or more abundant.*" Therefore, it has to move far enough to outrun diffusion. At typical diffusion constant D and speed v that minimum distance to outswim diffusion D/v is about 30 μm. It has been shown that this is just about what swimming bacteria were doing [11.33].

11.1.4 Reynolds Number for Diatoms

According to Edgar, the Reynolds number of a diatom $\mathbf{10 \cdot 10 \cdot 100\ \mu m^3}$ in volume, moving at 10 μm/s is in the region of 10^{-4}, which is very low. "*A low Reynolds number (<1) indicates laminar flow, because in that case the viscous forces predominate. Movement of diatoms in water therefore represents a highly viscous situation in which inertial forces are negligible, despite the fact that water itself is not a highly viscous liquid*" [11.16].

"*This means the diatom cannot 'coast' or 'freewheel'*" [11.36]. Once the driving force for locomotion ceases, the cell will stop almost immediately.

> "Movement is directional, the path taken corresponding fairly closely to the course of the raphe system—curved where the raphe is curved (e.g., some *Nitzschia* species with eccentric raphe systems), straight where the raphe is straight (e.g., *Navicula, Pinnularia*), and even sigmoid where the raphe is sigmoid (e.g., *Pleurosigma angulatum* (Quekett) W. Smith 1852)" [11.36].

> "Because of the low Reynolds numbers the movement of diatoms is jerky and once the driving force for locomotion ceases the cell will come to a rapid halt. Also, there is no obvious reason why a streamlined shape should reduce drag at such a low Reynolds number. Furthermore, the idea of jet propulsion as mechanism of locomotion can be rejected, because it would prove extremely inefficient in a viscous situation" [11.16].

However, streamlining can be important for attached diatoms in rapidly moving water [11.23].

11.1.5 Further Thoughts About Movement of Diatoms

Movement of raphid diatoms is generally only possible on solid surfaces [11.22]. "During movement, polysaccharide is secreted into the raphe slit and is present within the whole length of the slit. Also, a discontinuous trail of this material is left behind by the diatom as it moves" [11.36]. According to Hopkins & Drum "so far two motility mechanisms can be derived from the evidence given; these could work separately or together" [11.27].

1. "The expansion of the crystalloid body fibrils (presumed to be trail substance) by hydration in the raphe system and subsequent spiraling could give a propulsive force … when some of this material adheres to the substratum" [11.27].
2. "A propulsive force could be created by expulsion of materials by contraction of the fibrillar bundles under the raphe, and the direction of such a stream against the point of adhesion of the trail substance" [11.27].

Hopkins and Drum also argued that "criticism of mucus secretion as it was postulated by Lauterborn (1896), by Müller (1893, 1894), Hustedt (1930) and Fritsch (1935) on grounds of quantity alone, can be countered in two ways: The material as detected by the accretion of particles is very adhesive and its expansion on hydration substantial; the small production by numerous crystalloid bodies would support Lauterborn's contention. Secondly, diatoms do not move continuously unless disturbed [11.27]. In darkness motility is slowed down and stops after 4–24 hours depending upon species (Hopkins, 1963)" [11.27].

Round *et al.* [11.36] have summarized the work of Edgar *et al.*, who have outlined a hypothesis to explain the mechanism of motility based on ultrastructural observations of protoplast structure in the vicinity of the raphe and other pieces of evidence:

> "It is suggested that the motive force is generated by interaction between actin filaments and transmembrane structures which are free to move within the cell and raphe, but fixed to the substratum at their distal ends. The transmembrane structure presumably includes an ATPase and a protein able to make translational movements within the plasmalemma. [...] The transmembrane structure is itself connected to filaments of acid mucopolysaccharide, which can become attached to the substratum at their distal ends. Thus, as the transmembrane structures are moved along the raphe by their interactions with the bundles of actin filaments beneath [11.14], the cell moves relative to the substratum. Edgar and Pickett-Heaps [11.17] proposed that the flow of mucopolysaccharide along the raphe is made easier by a hydrophobic lipid coat over the silica of the raphe-sternum. When the mucopolysaccharide reaches the end of the raphe, it is detached from the plasmalemma at the helictoglossa and continues within the terminal fissure (if present) before being left behind as a sticky but ephemeral trail" [11.36].

These mucilage trails were examined using atomic force microscopy (AFM) by Wang *et al.* [11.44]. It was also shown that the mechanism of diatom locomotion as explained in the prevailing model by Edgar does not work at least for *Navicula* sp. because of many reasons, e.g., "the turning of diatom gliding, that was never tried to be explained using the Edgar model, but diatoms have been shown frequently turning when gliding" [11.44]. Therefore, the mechanism itself still remains unsolved.

11.1.6 Possible Reasons for Diatom Movement

The reason for movement among diatoms is not essentially clarified yet. The movements often seem random. Therefore, the benefits for the diatom are not obvious. Possible benefits could be:

- Optimization of light conditions: Many motile species show positive or negative phototaxis. Also, photophobia can be observed, where diatoms react to strong local variations of light intensity with reversal of the direction of movement.
- Periodic vertical movement of diatoms that inhabit sand deposits, especially in intertidal zones. These sediments can be disturbed by tides and currents, so diatoms move upwards to stay at the surface of the sediment (see review article Harper 1977 [11.45]).
- Looking for places with better nutrient concentration or other advantageous chemical proportions (chemotaxis). In the publication of Bondoc *et al.* [11.4] it is shown that *Seminavis robusta* moves towards a source of silica.
- Colonizing new habitats.
- Searching and approaching a partner for sexual reproduction [11.5].

All of the possible benefits above have a change in location in common. Observing the movement of some species, it can be doubted that locomotion is always the motivation for movement. *Cymatopleura elliptica* (Brébisson) W. Smith 1852 mostly slowly rotates around a vertical axis, scarcely making any headway, meaning that it hardly budges from the spot. Benefit could in some cases also have physiological backgrounds like regulation of energy balance [11.25].

11.1.7 Underwater Acoustics, Hydrophones

11.1.7.1 Underwater Acoustics

In gases and liquids acoustic waves are pressure waves that spread longitudinally. The acoustic speed $c_{G,L}$ is dependent on the temperature. The different values for air and water can be seen in Table 11.1.

Acoustic speed is much higher in liquids than in gases due to the greater bulk modulus K. The acoustic speed also increases with higher pressure [11.7]. This can be seen by considering the following general equation to determine the acoustic speed in any gas or liquid [11.29]:

$$c_{G,L} = \lambda \cdot f = \sqrt{\frac{K}{\rho}} \tag{11.7}$$

Table 11.1 Different values for the acoustic speed $c_{G,L}$ in air and water at different temperatures [11.7].

Medium	$c_{G,L}\left[\frac{\mathbf{m}}{\mathbf{s}}\right]$ at 0°C	$c_{G,L}\left[\frac{\mathbf{m}}{\mathbf{s}}\right]$ at 100°C
air	331.5	387.5
water	1402	1543

The following empirical formula can be used to determine the speed in water c_L with various parameters for temperature Θ in [°C], salinity s in [%] and depth d in [m] [11.29]:

$$c_L = \left(1492.9 + 3 \cdot (\Theta - 10) - 6 \cdot 10^{-3} \cdot (\Theta - 10)^2 - 4 \cdot 10^{-2} \cdot (\Theta - 18)^2 + 1.2 \cdot (s - 35) - 10^{-2} \cdot (\Theta - 18) \cdot (s - 35) + \frac{d}{61} \right) \frac{\mathrm{m}}{\mathrm{s}} \tag{11.8}$$

11.1.7.2 Hydrophones

A hydrophone is a measuring instrument that transforms the waterborne sound into an electrical voltage which is proportional to the sound pressure. That signal can then be measured. So it is basically the underwater equivalent of a microphone. Modern hydrophones are usually composed of piezoelectric ceramics. Piezoelectric materials generate a voltage in response to applied mechanical stress, which is in this case the pressure wave of an acoustic signal [11.35].

During previous work with hydrophones by Kratochvil and Pollirer the sounds from aquatic plants during photosynthesis were recorded. "Oxygen is emitted in the form of bubbles which are released from the stomata or small openings caused by injuries. [...] In the moment of escape the oxygen bubble emits a short single sound pulse, which can be recorded with a hydrophone. This acoustic side effect can be used to detect changes in the rate of photosynthetic processes" [11.30]. Cf. [11.19].

11.2 Methods

11.2.1 Estimate of the Momentum of a Moving Diatom

For further consideration of the movement of diatoms a rough estimate of momentum can be made as follows: Calculations are based on a hypothetical diatom $10 \cdot 10 \cdot 100$ µm³ in volume, moving at 10 µm/s as proposed by Edgar [11.16].

Therefore, the volume of our diatom is: $V = 10^4\,\mu\mathrm{m}^3 = 10^{-4}\,\mathrm{m}^3$.

The density of our diatom was roughly assumed to be somewhere in between the density of water and silicon dioxide:

Density of water: $\rho_w = 997\ \mathrm{kg/m^3}$
Density of silicon dioxide: $\rho_s = 2650\ \mathrm{kg/m^3}$
Density of our diatom: $\rho \approx 1500\ \mathrm{kg/m^3}$

Therefore, the mass is: $m = \rho \cdot V = 1.5 \cdot 10^{-11}\,\mathrm{kg}$
Moving with the speed $v = 10\ \mu\mathrm{m/s} = 10^{-5}\,\mathrm{m/s}$

With that information the momentum of one single diatom can be calculated in the following way:

$p = m \cdot v = 1.5 \cdot 10^{-16}\,\mathrm{kg \cdot m/s}$

11.2.2 On the Speed of Expansion of the Mucopolysaccharide Filaments

In the following section a model to estimate the sounds produced by a moving diatom was created. Through changing the different parameters any other source of sound can be simulated in the same way.

11.2.2.1 Estimation of Radial Expansion

Preliminary Remarks

It is assumed that the fibril has the shape of a cylinder and that there is a homogeneous distribution of mucopolysaccharide inside the fibril. There is evidence [11.10] that a fully hydrated fibril is hollow inside, which is not explicitly considered in the model.

The model parameter values as used for the mathematical model can be found in Table 11.2.

When water molecules pass through the surface of the fibril, they can move inside by diffusion. However, such a description reaches its limits with fibrils consisting of only a few molecules. If, however, a continuum model is used as an approximation, the movement of the water molecules inside the fibril can be described by diffusion. The binding to the polysaccharides requires a modeling of the concentration of unbound water and the degree of saturation with water by spatial scalar fields. The coupling of the equations leads to a reaction-diffusion equation. A high complexity results from the introduction of fibril expansion depending on the local bound and unbound water content. This probably requires very sophisticated modeling and simulation. This approach will not be pursued further here. In addition, the corresponding model parameters are not known.

Instead, an approximation method is used based on the assumption that the water molecules are bound very quickly and that there is a homogeneous water concentration within the fibril. Immediately after the fibril has been ejected and after saturation with water has been reached, this homogeneity is given. If one would take into account the fact that the water concentration at the surface is higher than inside, a slower water absorption and a slower increase of the radius would result. The following model calculation therefore overestimates the speed of expansion.

Table 11.2 Model parameter values with definition and sources as used for the mathematical model.

Parameter	Description	Values	Reference
r_0	initial radius of the fibril	2.5 nm	[11.10]
r_m	final radius of the fibril	12.5 nm	[11.10]
h	fibril length	0.3 to 3 μm (chosen: 3 μm)	[11.24]
k	mass transfer coefficient	$2.3 \cdot 10^{-5}$ m/s^{-1}	[11.41]
α	measure for mucilage expansion	4.7	[11.8]
R	distance between fibril and microphone	0.01 m	Equipment used

Model

The assumption is therefore the description by a water concentration c (in mol), which depends only on time. The flow on the surface of the fibril is proportional to the difference between the saturation concentration c_s and the concentration c:

$$j = k(c_s - c) \tag{11.9}$$

where k is the mass transfer coefficient (see [11.6]). Strictly speaking, concentration c applies only to the surface, but within the fibril.

The transfer through the entire surface A gives Aj. The change in the mass of water N (mol) inside the fibril is due to $Aj = \frac{dN}{dt}$:

$$\frac{dN}{dt} = \frac{d}{dt}Vc = Ak(c_s - c) \tag{11.10}$$

where the volume V of the fibril was introduced. As A and V are functions of the radius, Eq. (11.10) represents an equation with the time-dependent variables c and radius r. A second equation with these variables is provided by the equation (also used in [11.8])

$$V = V_d + \alpha V_w \tag{11.11}$$

where V_d is the volume of the fibril without water content ("dry") and V_w is the volume of the water in the water body, i.e., before hydration. For the factor α, $\alpha > 1$ (see [11.8]). The water is therefore not as densely packed in the bound state as in the bulk of the water. Eq. (11.11) is used (see Deng *et al.* [11.8]) for the case of complete hydration, so that V means the maximum volume ($V = V_M$). Obviously, the equation is also correct before the beginning of hydration ($V = V_d$). For volumes between the extremes, Eq. (11.11) would also apply, assuming that the inflowing water locally leads to complete hydration, so that an outer fully hydrated region and an inner water-free region exist. Since this cannot be assumed in principle, Eq. (11.11) is only considered to be a linear interpolation for all volumes.

For the volume of water it holds, $V_w = NV_M$, where V_M is the volume of one mole of liquid water. From Eq. (11.11) it follows:

$$N = \frac{V - V_d}{\alpha V_M} \tag{11.12}$$

Using Eq. (11.10) we get:

$$\frac{d}{dt}V = \alpha V_M Ak\left(c_s - \frac{V - V_d}{\alpha V_M V}\right) \tag{11.13}$$

An approximation was used that V_d is not time-dependent and that $c = N/V$. Until now, the geometric shape of the fibril was not explicitly taken into account. It is assumed that

the cylinder has a radius of r and the height of h. Water absorption should only take place through the curved surface area and expansion should only take place radially. If you insert $V = r^2\pi h$, $V_d = r^2\pi h$ and $A = 2r\pi h$ in Eq. (11.12), you get an equation with r as the only time-dependent variable ($dV/dt = Adr/dt$):

$$v = \frac{d}{dt}r = k\left(\alpha V_M c_s - \frac{r^2 - r_d^2}{r^2}\right) \tag{11.14}$$

If the radius of the cylinder without water content r_d and at saturation with water r_d are used as model parameters, c_s is not an independent parameter. From Eq. (11.12) we get results for saturation with water ($V = V_m$) and with $c_s = N/V$ (N total amount of water absorbed):

$$c_s = \frac{r_m^2 - r_d^2}{\alpha V_M r_m^2} \tag{11.15}$$

If $r_d \ll r_m$, then $c_s \approx 1/(\alpha V_m)$ is valid as expected. So far it has not been determined in which state the expansion will start. It should be assumed that the fibril initially contains no water, so that the start condition at time $t = 0$ is $r_0 = r(0) = r_d$ and $V_0 = V(0) = V_d$. With this definition and with Eq. (11.15), Eq. (11.14) it is taking the form:

$$v = \frac{d}{dt}r = k\left(\frac{r_0^2}{r^2} - \frac{r_0^2}{r_m^2}\right) \tag{11.16}$$

The initial velocity $v(0)$ results with $r(0) = r_0$ from Eq. (11.16) giving

$$v(0) = k\frac{r_m^2 - r_0^2}{r_m^2} \tag{11.17}$$

The calculation of the quantity $v(0)$ does not yet make use of the assumption of homogeneous water density in the fibril over the period of expansion, because this homogeneity is given at the beginning. A reaction-diffusion equation should also provide this initial value.

In [11.8] $k = 2.3 \cdot 10^{-5}$ m/s is used (adopted from [11.41]). Using the model parameters for r_m and r_0 (Table 11.1) it follows from Eq. (11.17):

$$v(0) = k \cdot 0.96 \approx 2.21 \cdot 10^{-5}\ \text{m/s} \tag{11.18}$$

If this speed would last until reaching the maximum radius (12.5 nm), this radius would be reached in 0.57 ms. This is very long compared to the estimated duration of the ejection, so that almost the entire expansion of the fibril takes place after the ejection. However, the form of Eq. (11.16) shows that the velocity decreases very rapidly with the radius. In the above approximation, at twice the radius of the starting value r_0 it is only 1/4 of the speed at the start.

Eq. (11.16) can be analytically integrated after separation of variables. The inverse function $t(r)$ reads:

$$t = k^{-1}\frac{r_m^2}{r_0^2}\left(\frac{r_\mathrm{m}}{2}\ln\frac{r_m + r}{r_m - r} - C_0\right) \tag{11.19}$$

with the integration constant C_0:

$$C_0 = -r_0 + \frac{r_m}{2}\ln\left(\frac{r_m + r_0}{r_m - r_0}\right) \tag{11.20}$$

Numerical Results

For the volume, the length of the fibril h is also needed (Table 11.1). From the range 0.3–3 µm the value 3 µm was chosen in order to describe the optimum case of observability. In Figure 11.1, the graphs according to Eq. (11.19) show the expected qualitative behavior:

In the selected time period, after a steep ascent, a slow increase of the radius is seen. The initial radius is doubled in approx. 0.284 ms. The doubling of the surface $\left(\sqrt{2}r_0\right)$ is already achieved after approx. 0.071 ms. The fast decrease of the speed with increasing radius leads to the fact that the 10-fold initial radius is never reached.

As the radius asymptotically approaches the maximum radius r_m, this radius is never matched. As a measure for the duration of the expansion, you can define, for example, after which time 90% of the radial expansion is completed. If the characteristic radius r_k is defined by $(r_k - r_0)/(r_m - r_0) = 0.9$ the characteristic radius is reached after $9.05 \cdot 10^{-3}$ seconds.

For the question of sound generation, it is important that rapid expansion only occurs as long as the radius of the fibril is a few nm.

11.2.2.2 Sound Generation

Model Assumption

One of the main assumptions was that the fibrils are ejected at an enormous speed and therefore their expansion along their entire length starts as soon as they are in the water

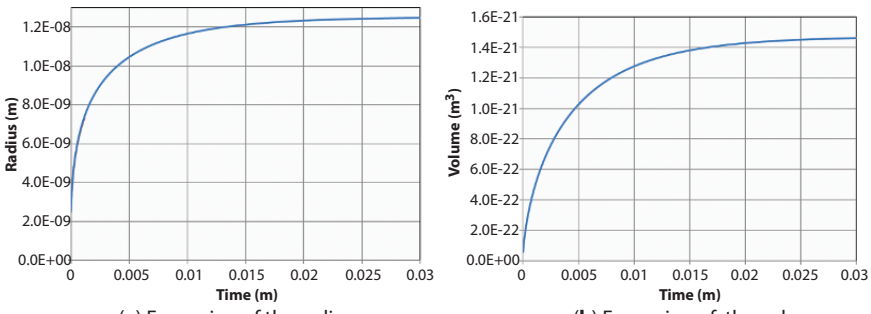

(**a**) Expansion of the radius (**b**) Expansion of the volume

Figure 11.1 Expansion of a cylindrical mucopolysaccharide fibril.

body. Apart from a possible sound development due to the ejection itself, the sound is generated by the expansion of the cylindrical fibril. This expansion starts with an initial velocity of $v(0) = 0.96 \cdot k$. With the selected model parameters, the expansion initially occurs at $2.21 \cdot 10^{-5}\,\mathrm{ms}^{-1}$. After that, the speed drops very rapidly. Therefore, a wide frequency spectrum can be expected. Theoretically it is infinitely broad according to the model; because the movement starts immediately, practically an infinitely steep edge is not to be expected in nature.

In the following estimation we therefore work with the assumption that the wavelengths of the sound are large compared to the expansion of the sound-emitting body. A wave of the wavelength of λ corresponds to a frequency of c_L/λ, where c_L is the speed of sound in water (about 1500 m/s). If we would consider frequencies where the wavelengths are in the range of the length of the fibril (0.3 to 3 µm [24]), we would also have to include frequencies in the range of $2.5 \cdot 10^8$ to $2.5 \cdot 10^9$ hertz.

Velocity Potential and Boundary Condition

When using a description of the sound by a velocity potential Φ, so that the velocity of the particles in the wave v_s is given by the gradient of this scalar potential

$$v_s = \nabla \Phi \tag{11.21}$$

the following equation must be solved:

$$\Delta \boldsymbol{\Phi} - \frac{1}{c_L^2} \frac{\partial^2 \boldsymbol{\Phi}}{\partial t^2} = 0 \tag{11.22}$$

Considering an expanding body with a solid surface, the normal component of the liquid velocity at the surface must be equal to the normal component of the velocity of the body at the surface [11.31]:

$$\frac{\partial \boldsymbol{\Phi}}{\partial n} = v \tag{11.23}$$

In the case of the expanding fibril, however, water from the water body flows into the fibril, which reduces the speed of the water pressed outwards, as shown in Figure 11.2.

Instead of Eq. (11.23) we write:

$$\frac{\partial \boldsymbol{\Phi}}{\partial n} = v - v_w \tag{11.24}$$

Here v_w is the velocity with which the water flows into the fibril. From Eq. (11.11) it follows that

$$\alpha \frac{dV_w}{dt} = \frac{dV}{dt} = A \frac{dr}{dt} = Av \tag{11.25}$$

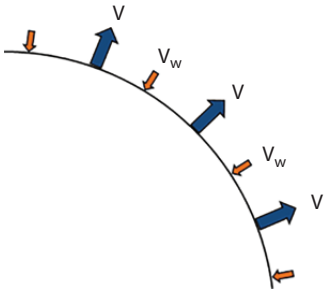

Figure 11.2 Schematic drawing of the expanding fibril.

As the volume change of the water is given by the flow of water through the surface ($dV_w/dt = Av_w$), the following applies:

$$v_w = A^{-1}\frac{dV_w}{dt} = \alpha^{-1}v \tag{11.26}$$

Eq. (11.24) therefore becomes

$$\frac{\partial \Phi}{\partial n} = v - v_w = \frac{\alpha - 1}{\alpha}v \tag{11.27}$$

Calculation of the Velocity Potential

In the vicinity of the body (distance small compared to the wavelength) the second term in Eq. (11.22) can be neglected and the Laplace's equation $\Delta\Phi = 0$ applies. In [11.31] it is shown that for large distances compared to the size of the body but small compared to the wavelength a general solution of the Laplace's equation exists which has the form

$$\Phi = -\frac{a}{R} + K\nabla\frac{1}{R} \tag{11.28}$$

R is the distance to the sound emitting object, where the coordinate origin is somewhere inside the body. The first term a/R only occurs when the body is pulsating, whereby $4\pi a$ represents the flow of liquid through a closed sphere around the body, so that

$$4\pi a = (v - v_w)A = \frac{\alpha - 1}{\alpha}vA = \frac{\alpha - 1}{\alpha}\dot{V} \tag{11.29}$$

By looking at the outgoing spherical wave ($R \gg l$), the solution for Eq. (11.22) is given:

$$\Phi = -\frac{\alpha - 1}{\alpha}\frac{\dot{V}(t - R/c_L)}{4\pi R} \tag{11.30}$$

and for the velocity of the particles in the wave

$$v_s = \nabla \Phi = \frac{\alpha - 1}{\alpha} \frac{1}{4\pi c_L R} \ddot{V}\left(t - \frac{R}{c_L}\right)\hat{n} \tag{11.31}$$

where $\hat{n}$ is the unit vector in radial direction. Eqs. (11.30) and (11.31) are adopted from [11.31], whereby only the pre-factor has been modified.

The factor $(\alpha - 1)/\alpha$) in Eqs. (11.30) and (11.31) shows that sound generation only occurs if $\alpha > 1$. If $\alpha = 1$, then the radius of the fibril would grow to its maximum size, but water would enter to the same extent as its diameter increases. An impulse would not be transferred to the surrounding water. As model parameter $\alpha = 4.7$ was used. Thus $(\alpha - 1)/\alpha \approx 0.79$. Altering this factor would not change the result by orders of magnitude.

Calculation of the Sound Pressure

For the question of which signal is produced by a microphone, the sound pressure of the pulse is determined.

$$p = \rho_0 c_L v_s \tag{11.32}$$

where ρ_0 is the density of the water. Using Eq. (11.31) one gets

$$p = \rho_0 c_L \frac{\alpha - 1}{\alpha} \frac{1}{4\pi c_L R} \ddot{V}\left(t - \frac{R}{c_L}\right) \tag{11.33}$$

By expressing the radius r in the solution $t(r)$ according to Eq. (11.19) by the volume V and deriving it with respect to V, one obtains:

$$\dot{V} = 2k\sqrt{\pi h}\frac{r_0^2}{r_m^2}\frac{V_m - V}{\sqrt{V}} \tag{11.34}$$

A second differentiation yields

$$\dot{V} = 2k\sqrt{\pi h}\frac{r_0^2}{r_m^2}\dot{V}\frac{\sqrt{V} + V_m/\sqrt{V}}{V} \tag{11.35}$$

where $\dot{V}$ is given by Eq. (11.34).

For a radius r with $r_0 \le r \le r_m$ (r_m is never reached) the time at which this given radius is achieved can be calculated with the help of Eq. (11.19). Furthermore, r also gives the volume V. Using Eqs. (11.34) and (11.35), the time derivatives of the volume can be calculated and finally, with Eq. (11.33), the desired pressure p.

Assuming a distance between sound source and microphone of $R = 1$ cm and with the model parameters given above, this leads to this time dependence of p (Figure 11.3):

The maximum pressure is about $6.24 \cdot 10^{-11}$ Pa. Since the retardation R/c_L in Eq. (11.33) does not play a role for a single pulse, the shift in the time axis is not shown.

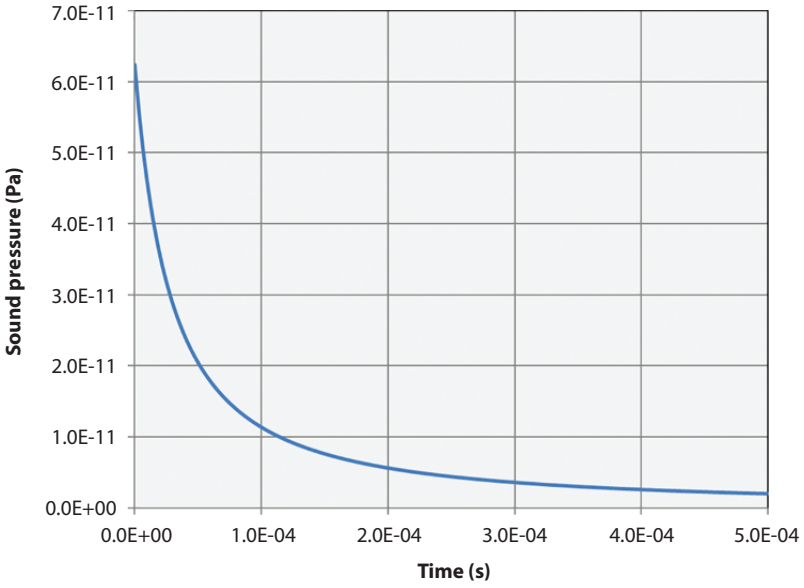

Figure 11.3 Time dependence of the sound pressure p.

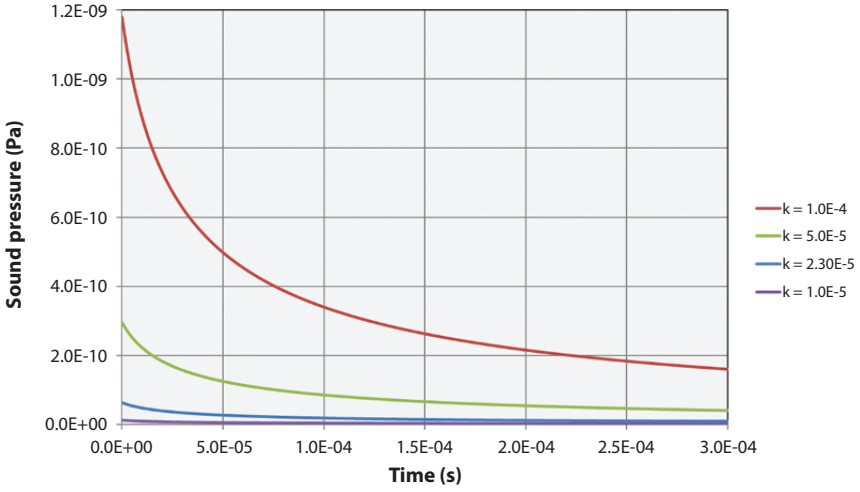

Figure 11.4 Time dependence of the sound pressure p for different mass transfer coefficients k.

It should be noted that the mass transfer coefficient k, which is not known exactly, has a large effect on $p(t)$. In Figure 11.4, in addition to the model parameter of $2.3 \cdot 10^{-5}$ m/s, other values covering one decade were used.

Finally, it should be mentioned that the sound absorption by the water has no relevant impact considering the small distances between diatoms and hydrophone. If a diatom moves on the substrate, however, the sound wave is created between the valve and the substrate. The sound can at least partially reach a hydrophone by diffraction around the valve (wavelengths in the detectable range are large compared to the diatom's extension). If the

raphe system opposite the substrate is active, a sound wave generated there can, however, propagate freely into the water body.

Note on Pulse Superposition and Sound Spectrum

For a single and a periodic pulse, its spectrum can be obtained by Fourier transformation. However, this is not of primary importance for observation with a hydrophone. A sequence of discrete single pulses can be recognized if the single pulse is perceptible by a "clicking" sound.[1]

However, if there are a lot of pulses per time, the probability of overlapping pulses increases. By superposition, higher pressures are then achieved than with a single pulse. With the pulse shape of $p(t)$ shown above, two pulses must follow in a time interval of no more than $1.81 \cdot 10^{-4}$ s, in order for the sum level to be about 10% above the maximum value of a single pulse. For a periodic pulse sequence, this is the case at 5500 pulses per second. As a rule, it can also be said for randomly distributed events that high pulse peaks rarely occur with significantly fewer than 5500 events on average per second. With a significantly higher number of pulses per time unit, one can profit from the superposition and achieve higher output voltages at the hydrophone. In Section 11.4 (Conclusions and Outlook) a pulse sequence of 400 pulses per second for a single diatom is estimated. These pulses should not overlap significantly in view of the short duration of the pulses. A positive effect on the observability beyond that of a single pulse can be expected from $5500/400 \approx 14$ active diatoms in the vicinity of the microphone. If the pulse sequence of a diatom is regular (no strong temporal fluctuations between single pulses), a clear peak in the spectrum at the frequency of the pulse sequence should be visible even in the case of many diatoms. Accordingly, this would show up in the autocorrelation function of pressure versus time.

11.2.3 Gathering Diatoms

Keeping diatoms is not that simple. Many species change their behavior when cultivated or kept in captivity because of the change in environment. Sometimes the diatoms even change their form. This can even lead to the point where the species cannot be identified anymore. If there is no sexual reproduction the diatoms get smaller and smaller until normally after a few months they are nonviable and the population dies out [11.39].

Nevertheless, there are a few raphid species that can be kept for years because they do not need sexual reproduction for a very long time, e.g., *Nitzschia palea*. That species is very active, durable, grows very fast and is therefore suitable and highly recommended for experiments. Other active species are diatoms from the *Navicula* genus. *Pinnularia* are also a suitable option, although they are rather sedate in their movement [11.39].

Edgar stated that: "Observations show that the large, bulky cells (e.g., *Pinnularia*, *Cymatopleura*) move more slowly than the flatter species (e.g., many *Navicula* spp. and *Nitzschia* spp.)" [11.16].

In order to keep diatoms, it is important that there is not too much water over the layer of diatoms in the container (as seen in Figure 11.5) to enable gas exchange also with the container closed, e.g., during transport. Of course, not closing the container airtight can be

[1] This can be compared to the observation of raindrops by the sound of their impact on a roof, which are statistically independent and produce a so-called shot noise. However, the pulses of a single diatom are not statistically independent.

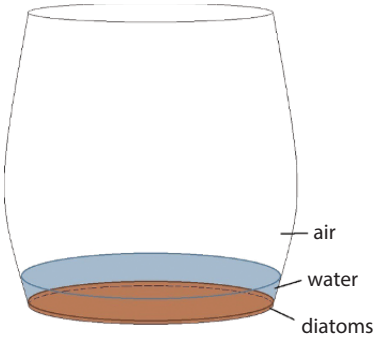

Figure 11.5 Schematic drawing of a jar with diatoms.

the preferred option, but it should be covered lightly to prevent entry of foreign substances or organisms from contaminating the water. Many diatoms can live well at a temperature of about 20°C. The container with the diatoms should ideally be placed at a window facing north, because direct sunlight should be avoided [11.39].

In general, there are two different ways of obtaining diatoms: Purchasing diatoms and catching diatoms in the wild. Both have advantages and disadvantages

11.2.3.1 Purchasing Diatom Cultures

Diatoms can be purchased online. As mentioned before, it should be considered that many diatom cultures that are kept in captivity for longer periods of time lose their typical morphology. Nevertheless, the advantages are that only one specific species can be obtained and the amount of foreign substances and organisms would be minimal.

At the University of Göttingen (Germany) there is an institution for research and cultivation of diatoms, where some species are offered. See also [11.38] [11.43].

11.2.3.2 Diatoms from the Wild

One advantage of diatoms that are harvested from the wild is that they are generally more active and vital. On the other hand, one disadvantage is that there are many different species and so it is hard to determine the one at hand. Single diatoms of the desired species can be extracted with capillary pipettes, but the species would first need to be identified. Another option to isolate raphid, motile diatoms could be to set a light spot to one area (perhaps on a microscope slide), so that motile diatoms would move there [11.39]. Redfern has already described another method to isolate *Navicula* and other test objects, using fine hairs [11.34].

Further research and experiments were made with diatoms from the wild exclusively (as shown in Figure 11.6.), because of their activeness and the possibility of obtaining them easily with little time investment, and performed some quick, rough measurements.

For gathering diatoms from the wild, a few different techniques were tried out:

Mud from the Bottom of a Body of Water

Because they can be found in almost every water body, diatoms can be obtained just by collecting mud, sand or other kinds of substrates from the bottom. For collecting raphid

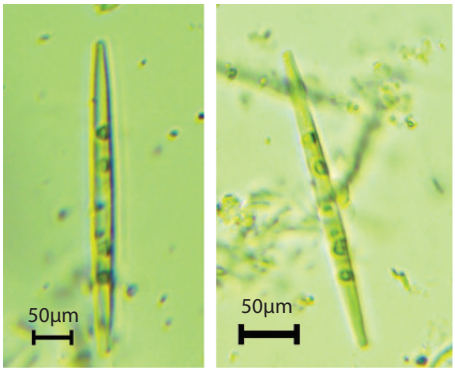

Figure 11.6 Raphid diatom (to our best knowledge), caught by FZ; Note the visibility of the chloroplasts inside the diatoms; the scale bars are estimated.

diatoms, it is advised to do so on the side of a river or creek, where the current is not too strong, but strong enough for non-raphid diatoms to get flushed away. In the case presented here, the mud from a pondside was collected in Natschbach, Austria on June 14, 2019 and observed under the optical microscope.

Placing a Substrate in a Water Body

Another option specifically for gathering raphid diatoms is to place some kind of substrate for diatoms to move up to in some body of water. Therefore, different kinds of substrates were placed in a small creek in Natschbach, Austria, with not too strong current and left there for a few weeks. This was done first with microscope slides and then with plastic foil, which could later be crumpled up to increase the surface of the substrate and thereby also the density of raphid diatoms.

Stones from Underwater

For this technique stones from underwater are collected. Stones with golden-brown film on them usually work well for obtaining diatoms (as displayed in Figure 11.7.). The film is brushed off into a container with an old toothbrush and then washed away with a little bit of water from the same origin as the diatoms. The water should then be of a light-brown color. To receive diatoms, only the film from the upside of the stone needs to be scraped off. This is also a technique specifically for gathering raphid, motile diatoms [11.9].

Comparison of the Different Methods

Samples of diatoms collected with the different methods were observed under an optical microscope from Budapest Telescope Center (BTC), model BIM313T.

In Figure 11.8a there are diatoms that were brushed off stones from underwater. This has proven to be the best method for obtaining raphid diatoms while at the same time mostly avoiding other organisms, plants or material. It can clearly be seen that there is the least amount of foreign substances.

Figure 11.8c shows mud from the edge of a pond. In this case, although many raphid diatoms were collected, many other organisms could also be observed.

On the right side of Figure 11.8, substrates that were placed in a small creek and left there for a few weeks are shown. Here the enormous growth of algae is clearly visible.

Figure 11.7 Stones from underwater with golden-brown film on them, collected by FZ in Natschbach, Austria, on May 5, 2019.

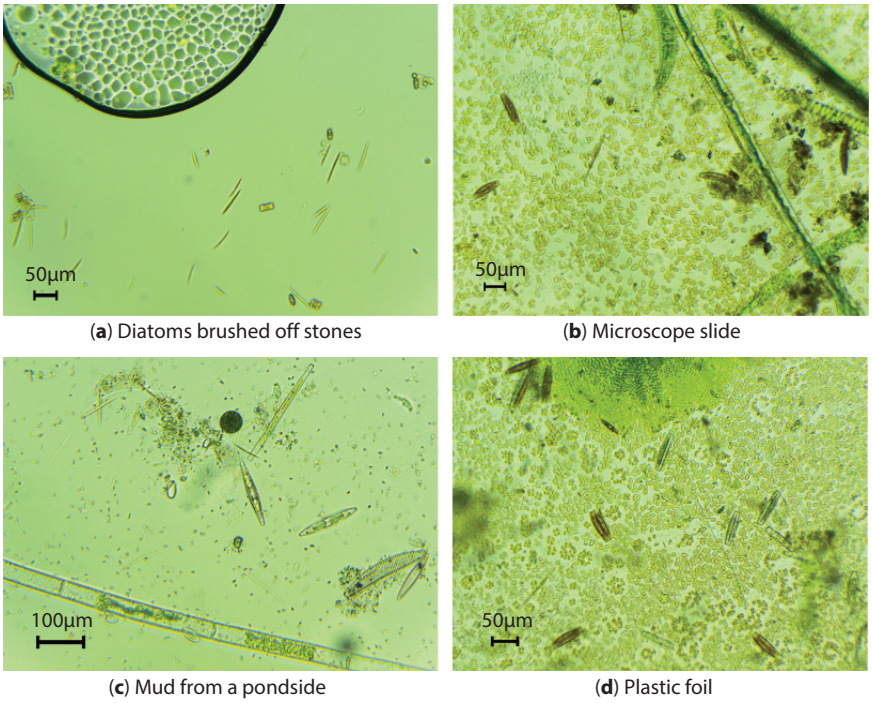

(**a**) Diatoms brushed off stones (**b**) Microscope slide

(**c**) Mud from a pondside (**d**) Plastic foil

Figure 11.8 Comparison of diatom samples obtained with different methods; the scalebars are estimated.

In Figure 11.8b, the substrate was a microscope slide made out of glass, which usually is a good substrate for raphid diatoms. Therefore, this sample contained many raphid diatoms, but also a lot of foreign substances.

In Figure 11.8d, the substrate was a piece from the plastic foil that was placed in the creek. Here the ratio of raphid diatoms to foreign substances is the worst of all methods that were used. Pennate diatoms usually cannot stick well to plastic, so plastic is not a suitable substrate.

11.2.4 Using a Hydrophone to Detect Possible Acoustic Signals from Diatoms

11.2.4.1 First Setup

For a first measurement, to detect possible acoustic signals related to diatom movement, diatoms were first scraped off stones from underwater and then mud and sand from a

riverside were collected. For every measurement with diatoms, a reference measurement was performed. It is important that the reference container is of the same material and shape as the container with diatoms. Furthermore, it was filled with water from the same origin as the diatoms, directly from the top of the small creek, where the water is pumped from the bottom of the pond. Therefore, there probably were not that many live diatoms as in the containers where diatoms were gathered with the different methods presented earlier. The two containers had roughly the same level of liquid. The containers used were glass jars with a diameter of about 10 cm.

In Figure 11.9 the setup for these measurements is shown. On the left there is the power supply for the hydrophone, in the middle the recorder and on the right the jar with diatoms and the hydrophone and the reference jar. Here the diatoms scraped off stones are recorded. Also, different materials to muffle ambient noise can be seen in Figure 11.9. Usually textiles or artificial fur work well. In this case, vibration-insulating mats (as seen in yellow) were also used. The material these mats are made from is called "Sylomer" from Getzner Werkstoffe GmbH in Vorarlberg, Austria. There are different kinds available for different weight forces (force per area).

The hydrophone used was a Brüel & Kjær hydrophone, Type 8106, with the hydrophone power supply also from Brüel & Kjær, Type 2804. The recorder used was a Tascam DR-100 MKIII linear PCM recorder. This hydrophone Type 8106 is a low-noise hydrophone, designed for the measurement of weak, underwater signals. It has a frequency range from 3 Hz to 80 kHz and a receiving sensitivity of −173 dB re 1 V/µPa. The measurements with the first setup were performed in an office with a surrounding background sound level of 39 dBA, re 20 µPa, RMS fast, where "dBA" means "decibel according to evaluation curve A," which takes into account the human hearing, "re" stands for "relative to." So "relative to 20 µPa" is the sound pressure reference value in the level measurement, which corresponds to the human hearing threshold at 1000 Hz. This has to be stated in this context, because it specifies the reference level. Otherwise, this declaration would be ambiguous. "RMS fast" means that the measuring steps were performed at intervals of 135 ms.

Figure 11.9 Setup of first measurements.

Figure 11.10 Measurement of jar with diatoms (right), reference jar (left).

Figure 11.10 shows the measurement of the diatoms that were collected from a river, together with mud, sand and possibly many foreign organisms and substances. Nevertheless, a rough measurement was performed.

11.2.4.2 Second Setup

In a second attempt, we tried to increase the density of raphid diatoms. To do so, transparent glass balls with a diameter of about 4 mm [11.3] were filled in jars so that the bottom was covered with them. The glass balls are made from soda-lime glass, the prevalent type of glass.

Diatoms were collected by scraping them off stones from the same creek as before and put inside the jars with the glass balls, as seen in Figure 11.11. For the measurements, the content of all the jars could be filled in one container, and with the much higher surface there would hopefully also be a higher density of raphid diatoms. A reference jar with roughly the same amount of glass balls and the same level of water from the same creek was also prepared.

The hydrophone and its power supply were the same as in the first setup, but the recorder was a Marantz model No. PMD660.

Additionally, we tried to record the noises made by two adult great pond snails—*Lymnaea stagnalis* (Linnaeus, 1758). These animals have a radula, which they use to scrape algae off a surface and eat them. This usually produces a munching sound. The snails were put in an extra jar with water from the same origin. The rest of the setup remained the same as for the diatoms.

This time measurements were performed in a soundproof room in Althanstraße 14, 1090 Vienna, Austria. Its internal dimensions are 3 m · 3 m · 3 m. Beyond there is 1 m of silencers

Figure 11.11 Jars with diatoms and little glass balls.

out of foam material on the ceiling, on the floor and on all four walls. Behind that there is a double wall filled with sound-insulating material. The whole cube is mounted on buffers out of rubber and also acts as a Faraday cage. At the time of the measurements 3 observors were present in the room, which could have been an additional source of noise, but was considered neglectible, as the goal was only to perform rough measurements.

11.3 Results and Discussion

11.3.1 Spectrograms

Figures 11.12 and 11.16 show the results of the setup shown in Figure 11.10 and the results of the reference measurement with the same water but without diatoms. The diagrams shown here are spectrograms, the illustrations of the frequency spectrum of a signal, as they are used for analysis of acoustic signals. They serve as an overview illustration of sound signals and cannot be used to read exact amplitude values. On the abscissa the time in [s] and on the ordinate the frequency in kilohertz [kHz] is displayed. The sound level in decibel [dB] is displayed through color, where brighter colors indicate stronger sound levels. In the following spectrogram, 40 dB are displayed (−82 dB…−42 dB). This makes 0.634 dB per color grade. The color range is ordered as follows: black (≤ −82 dB), dark blue, light blue, green, yellow, white, red (≥ −42 dB). Exact values and differences in the sound levels can be read off the averaged spectra.

All averaged spectra were created in the same way. For each of the two recordings a long-term averaging and a short-term averaging were performed. Comparing the short- and long-term averaged spectra shows that the spectrum is quite stable over the whole period of time (short converges to long). Also, besides short disturbances or pulses, no recognizable signal is visible. Differences between the averaged spectra of the two recordings can be

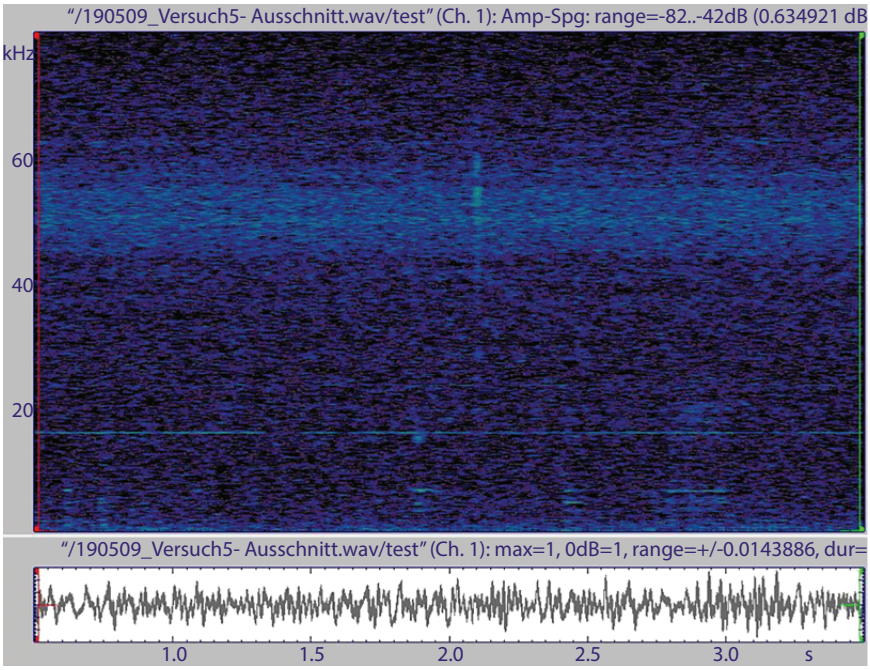

Figure 11.12 Spectrogram of measurement with diatoms.

explained as follows: Firstly, it is a matter of two recordings that were performed separately. Secondly, the recordings have different lengths and the pulses are not evenly distributed. Lastly, the horizontal lines in the spectrogram/peaks in the spectrum differ, showing the same frequency but different sound levels.

Analyzing the recorded sounds and creating the spectrograms was done with the program STx. It is freeware and can be downloaded from the website of the Austrian Academy of Sciences [11.2].

Some characteristics of the spectrogram of the measurement with diatoms (Figure 11.12) can be summarized as follows:

Throughout the whole signal:

- Tone at 16.4 kHz, 10 dB above the background
- Tone at ca. 24 kHz, 7 dB above the background (occasionally interrupted or AM modulated)
- Noise band between 44 kHz and 64 kHz

At some locations:

- Tone at ca. 7200 Hz, slightly modulated; The level is difficult to measure, ca. 3–8 dB above the background. For example, between 2.75 s and 3 s: a tone at about 7100 Hz (+8 dB) and a modulated/varying tone between 4800 Hz and 5200 Hz
- There are similar signals between 2.4 s – 2.5 s and 1.85 s – 1.95 s and possibly 0.6 s – 0.95 s.

In Figure 11.13, both stationary tones (16.4 kHz and 24 kHz) and the noise band are clearly visible. The small peaks at around 5 kHz and 7 kHz are caused by the sporadic signals.

In Figure 11.14 the stationary tone at 16.4 kHz and the localized tone at ca. 7100–7200 Hz are clearly visible.

In this range (Figure 11.15) there is no occurrence of the sporadic tones, and the spectrum is therefore similar to the averaged spectrum over the whole signal (Figure 11.13), although the variance is higher, since the averaged signal is shorter. The same kind of considerations were made for the reference measurement.

Throughout the whole signal:

- Tone at ca. 16.4 Hz, 13 dB above the background
- Tone at ca. 24 kHz, 7 dB above the background (occasionally interrupted or AM modulated)

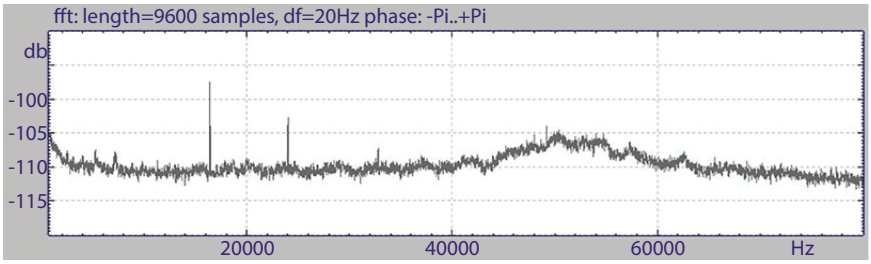

Figure 11.13 Averaged spectrum over the whole spectrogram (0.5 s – 3.5 s).

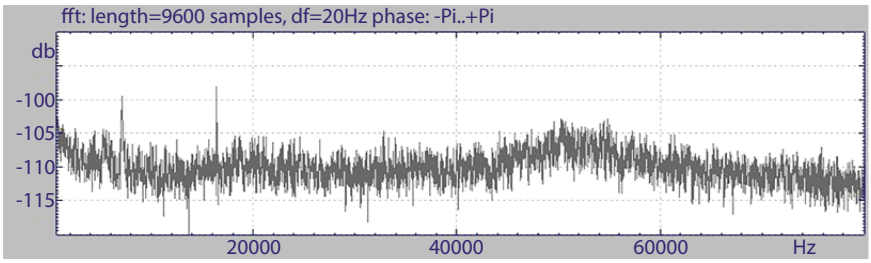

Figure 11.14 Averaged spectrum over the range 2.75 s – 3 s.

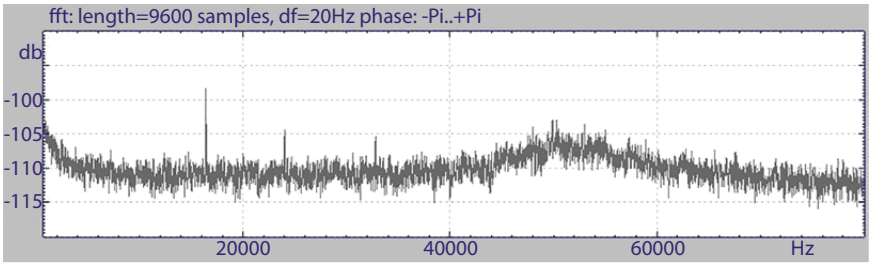

Figure 11.15 Averaged spectrum between 1 s – 1.5 s.

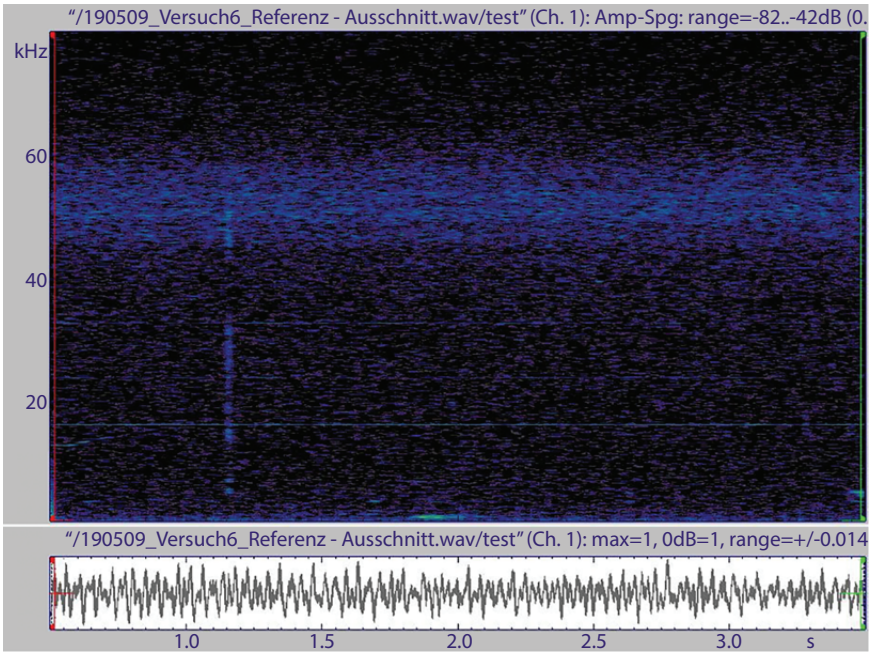

Figure 11.16 Spectrogram of reference measurement.

- Tone at ca. 32.8 Hz, 10 dB above the background
- Noise band between 44 kHz and 64 kHz

At some locations:

- At ca. 1.2 s there is a short broadband disturbance.
- At ca. 1.65 s – 1.75 s (just before the relative strong 1.3 kHz tone) there is a short tone at ca. 4000 Hz (possibly with parts at lower frequencies).

Comparison with the first signal of the measurement with diatoms:

- All three tones are also present in the first sound file (Figures 11.12–11.15), though with lower amplitudes (particularly the 32.8 kHz tone).
- The tones at 7 kHz and 5 kHz found in the first sound file are not found here.

In Figure 11.17 the three static tones (16.4 kHz, 24 kHz, 32.8 kHz) and the noise band are clearly visible.

In Figure 11.18 a tone with slowly rising frequency can be seen at ca. 12.5 kHz to 13.5 kHz.

Figure 11.19 shows a relatively strong tone at ca. 1300 Hz (not completely stable frequency).

Figure 11.20 shows only the "background signal." It is similar to the average of the complete signal, but with higher variance.

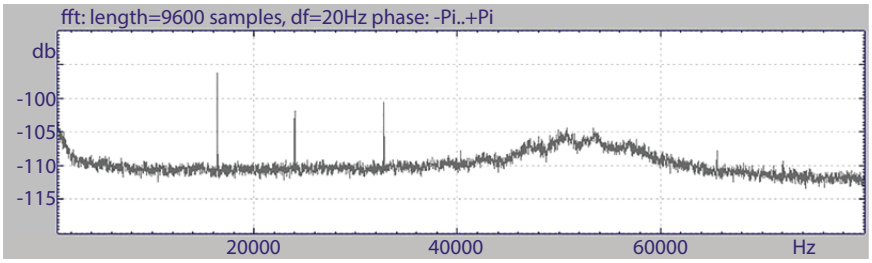

Figure 11.17 Averaged spectrum over whole spectrogram (0.5 s – 3.5 s).

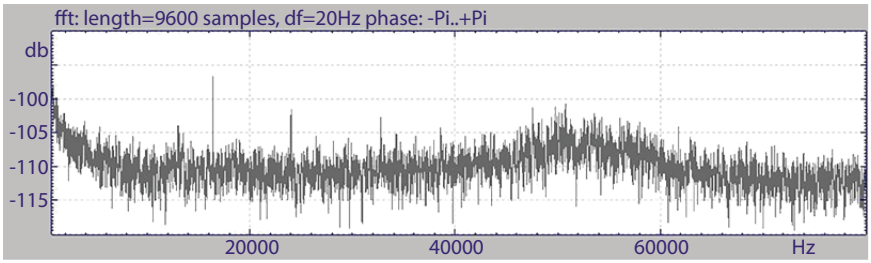

Figure 11.18 Averaged spectrum between 0.5 s – 0.65 s.

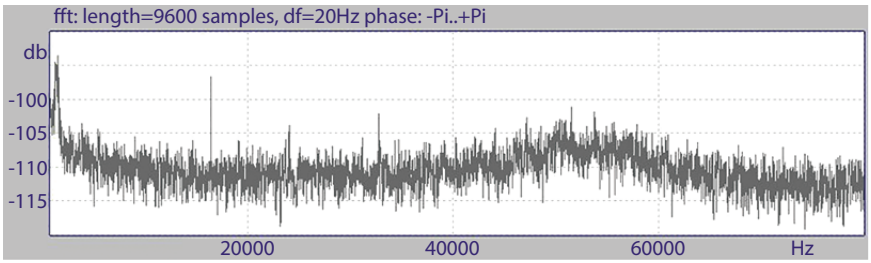

Figure 11.19 Averaged spectrum between 1.85 s – 2 s.

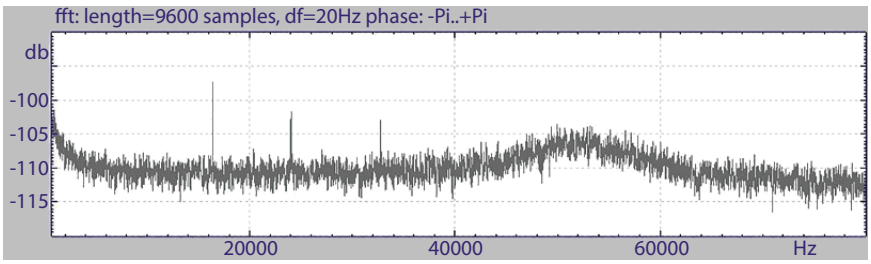

Figure 11.20 Averaged spectrum between 2.5 s – 3.0 s.

Apart from background noise in both measurements no sounds could be recorded. The spectrograms of the measurements with diatoms and the reference measurements show no great differences. They also do not look exactly the same, which is due to the fact that they were not recorded at the same time, which would require two

hydrophones. The recordings of diatoms scraped off stones, as well as the measurement of the containers with diatoms on glass balls, all led to the same results.

The recordings of *Lymnaea stagnalis* were a challenge, because they did not seem to be very hungry at the time of the experiment. Only one quiet munching sound could be recorded. For this experiment with the snails, it might be best to put the hydrophone under water for some time, so that algae can grow on it. Then the snails could scrape them right off the hydrophone, which would produce a strong signal.

11.3.2 Discussion

At the Institute of Sound Research of the Austrian Academy of Sciences, the comparative sound recordings (with diatoms and reference recording without diatoms) were subjected to a detailed analysis. Averaged spectra were taken from equally long sections of both signals. These showed background signals that could not be distinguished between the two signals. Stable partials that occur in the background have the character of technical faults. Likewise, faults are to be detected, but these occur only for a short period of time and therefore cannot originate from the expected organic source.

In summary, it can be stated that both recordings have a very similar background signal, which is present over the entire time. This can be shown by the overall average spectra (Figures 11.12 and 11.16) and by the short-time averages (Figures 11.15 and 11.20), which have the same mean but a higher variance (because of the shorter average time). The first recording (measurement with diatoms) contains some short localized signals with low frequency components. Because the signals have similar frequency components, they may be caused by the same (probably mechanical) source. The second recording (reference measurement) also contains some short low-frequency signals, but they are different from that in the first signal. The stable/continuous tones at 16.4 kHz, 24 kHz and 32.8 kHz are probably caused by electrical devices (monitor?).

The results from these experiments could have different causes. It is possible that there simply were not enough diatoms. For recording sounds with hydrophones, it would be best if the diatoms stuck directly to the surface of the hydrophone and move alongside it. This is not very likely because most hydrophones usually are coated with elastomers, which is probably not a suitable substrate for raphid diatoms.

Furthermore, the sounds of the diatoms could also be too quiet to be recorded with that kind of hydrophone. The problem here is that hydrophones need to be of a certain size to be very sensitive. At the same time, it would be best to get as close to the diatoms as possible, which would require a small hydrophone, but with smaller size its sensitivity decreases.

Finally, it is also possible that there simply are no sounds related to raphid diatom movement.

11.4 Conclusions and Outlook

We have put forward the hypothesis that diatoms are driven by the explosive hydration of the mucopolysaccharide microfilaments released from raphes, whose diameter may be estimated from micrographs in [11.13] at 50 nm. If a diatom is moving at 20 μm/s, it would then be releasing 20,000/50 = 400 filaments per second. If these are indeed explosions, they would then be occurring in the frequency range of 0.4 kHz. However, an individual explosion could

last for an even shorter period of time. If a filament exits the raphe at the speed of a discobolocyst (a projectile launching organelle), estimated at 260 m/s [11.21], and we assume a filament length equal to the cross-sectional length of a raphe (0.3–3 μm in [11.24]), then a single explosion could last as little as 1 ns, providing acoustic frequencies in the range of 10^6 kHz. The latter is beyond the frequency range of the hydrophone we used and might explain our negative result. There is a possibility that the diatom trail itself damps the sound of hydration explosions, as analogously suggested for instrument vibrations [11.37].

Of course, all the experiments performed were rough, basic approaches and could be refined tremendously. With two hydrophones of the same kind available, the reference measurement could be done at the same time as the measurement of the jar with diatoms. Then the signal of the reference measurement could be subtracted and only sounds that are present in the jar with diatoms would be shown, assuming that the noise is from the environment or the observer and not from the hydrophone itself. A soundproof room is possibly the best environment to perform these kinds of measurements, but with two hydrophones it might not be necessary, because most of the background noise would be cancelled out.

Another issue is the density of diatoms, which should definitely be increased, because the more diatoms per volume unit there are in the container, the more likely it is to detect possible sounds. To accomplish that, while at the same time maintaining the diatoms' activeness, it could be worth trying to put active, vital diatoms from the wild into one container together with great numbers of diatoms from cultures. Increasing the surface could also be done by constructing some kind of inset out of microscope slides, or, even more ideally, coverslips on which the diatoms could attach. Because coverslips are made out of very thin glass, they would amplify potential vibrations.

The glass balls that were used to increase the surface (as presented in Subsection 11.2.4.2), are out of solid glass. A proposal to improve the experiment would be to use hollow glass balls, like Christmas tree balls, but much smaller. Of course, they would float on the water because of buoyancy, and therefore would have to be held underwater, e.g., with a net or sintered or glued to a surface.

Another promising approach could be to experiment with colonies of *Bacillaria*, the earliest known genus of diatoms. *Bacillaria* cells live in colonies where the cells are connected to long strands and can move parallel to each other [11.28]. This would provide a high density of diatoms, which means higher sound levels can be expected. Sounds could also occur in *Diatoma* colonies. This genus forms chains or even bundles and sometimes two parallel diatoms open up to form a "V" so that the chain reaches a new state of equilibrium. This process happens very fast and could possibly produce an acoustic signal.

A suggestion for a setup for future measurements would be to grow a very dense colony of diatoms, preferably of a species that is very active. Ideally, they are bred directly on the hydrophone, because the acoustic signal would decrease tremendously with increasing distance. Then possible changes in the signal could be detected when the light is turned off and on again, because diatom movement is in most cases correlated with light intensity.

An alternative proposal to the presented method could be to use a vibrometer. A drop of water with diatoms would have to be applied onto a very thin bar, e.g., an AFM cantilever, which could maybe be stimulated by the vibrations of the diatoms. This could be measured via interference. Of course, a reference measurement with the same amount of water but without diatoms would also have to be performed.

As another approach an optical hydrophone could be used, e.g., from XARION Laser Acoustics GmbH in Vienna. Their hydrophone output signal is analogue (max ±7.5 V at 50 Ohm), therefore there is no software, but it can be connected with any measurement device. According to Wolfgang Rohringer, the lowest sound pressures detectable at the moment are at ~ 50 μPa/Hz, in a frequency range from 10 Hz to ~ 3 MHz.

In case acoustic analysis of diatoms succeeds in the future, an interesting application could be to track the sounds of different activities in water, especially of moving diatoms. Through that perhaps conclusions about diatoms or other active organisms inside the water body could be made.

Acoustic methods for analysis and control of friction processes are widely used in tribology. Approaches on triboacoustic monitoring of friction were made by Dykha *et al.* [11.12] [11.11]. There have already been proposals to measure vibrations with MEMS (microelectromechanical systems) sensors, e.g., by Looney. The sounds produced by the repetitive mechanical motion of mechanical parts can be used to observe machine health [11.32].

If measuring low intensity sound signals of that kind succeeds, it could be applicable to ensure the proper functionality of machines. The measured acoustic signals could serve as a check if a device is working correctly [11.40] [11.20].

We hope that these rough initial measurements of sounds of underwater creatures will stimulate further research along these lines, and that future scientific approaches can build upon our undertakings! Shrimp and other marine organisms produce and use sound that propagates distances many times their sizes. Perhaps there is yet a definitive chapter on diatom ecoacoustics [11.18] to be written.

Acknowledgements

FZ: I am very grateful for all the wonderful people around me, who provided me with the motivation to carry on through all the different work stages and supported me especially when things seemed to be stuck.

During the past year I worked on this subject with Alexander Müller. We did a lot of research, developed many ideas and also performed the measurements together. Thank you for that!

A big thank you goes out to my parents who luckily decided to build a pond in the garden many years ago which provided me with a sheer inexhaustible source of vital diatoms to play with.

I would really like to express my gratitude to Wolfi Murnberger who provided his optical microscope and spent a lot of time with me, watching the mesmerizing gliding movement of diatoms. I also want to thank Michael Schagerl, Manfred Kaltenbacher and Michael Kloster for the helpful communications per email and/or in person.

References

[11.1] Alicea, B., Gordon, R., Harbich, T., Singh, A., Varma, V., Mehan, P., Singh, U., Machine learning segmentation of diatom movies: Towards a digital *Bacillaria paradoxa* [BCLA], in:

Diatom Gliding Motility [DIGM, Volume in the series: Diatoms: Biology & Applications, series editors: Richard Gordon & Joseph Seckbach] [In preparation], S.A. Cohn, K.M. Manoylov, R. Gordon (Eds.), p. #s, Wiley-Scrivener, Beverly, MA, USA, 2020.

[11.2] Austrian Academy of Sciences Acoustics Research Institute, Sound tools extended (stx) - intelligent sound processing, URL https://www.kfs.oeaw. ac.at/stx/ (last accessed on 2021/01/14), 2020.

[11.3] Bastelwelt Creativ, Glaskugeln mini, klar, leicht bläulich schimmernd, 4 mm, 100 gr.„ URL https://www.bastelweltcreativ.de/glaskugeln-mini- klar-leicht-blaeulich-schimmernd/p-8760.html (last accessed on 2021/01/14), 2019.

[11.4] Bondoc, K.G., Heuschele, J., Gillard, J., Vyverman, W., Pohnert, G., Selective silicate-directed motility in diatoms. *Nat. Commun.*, 7, 10540, 2016.

[11.5] Bondoc, K.G., Kiel, C., Vyverman, W., Pohnert, G., Searching for a mate: Pheromone-directed movement of the benthic diatom seminavis robusta. *Microb. Ecol.*, 72, 2016.

[11.6] Cussler, E., *Diffusion: Mass Transfer in Fluid Systems, Cambridge Series in Chemical Engineering*, pp. 237–273, Cambridge University Press, Cambridge, England, 2009.

[11.7] Demtröder, W., *Experimentalphysik 1*, Springer, Berlin, Germany, 2005.

[11.8] Deng, W., Jeng, D., Toorop, P., Squire, G., Iannetta, P., A mathe- matical model of mucilage expansion in myxospermous seeds of capsella bursa- pastoris (shepherd's purse). *Ann. Bot.*, 109, 419–427, 2012, www.aob.oxfordjournals.org.

[11.9] diatomp, Diatomeen Teil 1: Einführung and das Sammeln von Diatomeen, URL https://www.youtube.com/watch?v=KOFd_EDAIeQ (last accessed on 2021/01/13), 2019.

[11.10] Drum, R.W. and Hopkins, J.T., Diatom locomotion: An explanation. *Protoplasma*, 62, 1–33, 1966.

[11.11] Dykha, A., Zaspa, Y., Slashchuk, V., Triboacoustic control of fretting. *J. Frict. Wear*, 39, 169–172, 2018.

[11.12] Dykha, A., Zaspa, Y., Vychavka, Y., Tribo-acoustic analysis of the processes of dynamic friction, *MOTROL. Comission of Motorization and Energetics in Agriculture*, vol. 19(2), pp. 11–14, 2017.

[11.13] Edgar, L., Mucilage secretions of moving diatoms. *Protoplasma*, 118, 44–48, 1983.

[11.14] Edgar, L. and Zavortink, M., The mechanism of diatom locomotion. II: Identification of actin. *Proc. R. Soc London Ser. B, Biol. Sci. (1934-1990)*, 218, 345–348, 1983.

[11.15] Edgar, L.A., Diatom locomotion: Computer assisted analysis of cine film. *Br. Phycol. J.*, 14, 1, 83–101, 1979, URL https://doi.org/10.1080/00071617900650111.

[11.16] Edgar, L.A., Diatom locomotion: A consideration of movement in a highly viscous situation. *Br. Phycol. J.*, 17, 243–251, 1982.

[11.17] Edgar, L.A. and Pickett-Heaps, J.D., The mechanism of diatom loco- motion. I. @ an ultrastructural study of the motility apparatus. *Proc. R. Soc London Ser. B, Biol. Sci.*, 218, 1212, 331–343, 1983, URL http://www.jstor.org/stable/35706.

[11.18] Farina, A., Ecoacoustics: A quantitative approach to investigate the ecological role of environmental sounds. *Mathematics*, 7, 1, 21, 2019.

[11.19] Freeman, S., Freeman, L., Giorli, G., Haas, A., Photosynthesis by marine algae produces sound, contributing to the daytime soundscape on coral reefs. *PloS One*, 13, 10, e0201766, 2018.

[11.20] Geisel, T., *Horton hört ein Hu!*, Rogner und Bernhard bei Zweitausendeins, Hamburg und Affoltern a. A., 2003.

[11.21] Gordon, R., A retaliatory role for algal projectiles, with implications for the mechanochemistry of diatom gliding motility. *J. Theor. Biol.*, 126, 4, 419–436, 1987, URL http://www.sciencedirect.com/science/article/ pii/S0022519387801492.

[11.22] Gordon, R., The whimsical history of proposed motors for diatom motility, in: *Diatom Gliding Motility [DIGM, Volume in the series: Diatoms: Biology & Applications, series editors: Richard Gordon & Joseph Seckbach]*, S.A. Cohn, M. Manoylov, R. Gordon (Eds.), p. #s, Wiley-Scrivener, Beverly, MA, USA, 2021.
[11.23] Gordon, R., Björklund, N., Robinson, G., Kling, H., Sheared drops and pennate diatoms. *Nova Hedwigia*, 112, Festschrift for Prof. T.V. Desikachary, 287–297, 1996.
[11.24] Gordon, R. and Drum, R., A capillarity mechanism for diatom gliding locomotion. *Proc. Natl. Acad. Sci. U. S. A.*, 67, 1, 338–334, 1970.
[11.25] Harbich, T., Introduction to motility, URL https://diatoms.de/en/diatoms/introduction-to-motility (last accessed on 2021/01/14), 2019.
[11.26] Harper, M. and Harper, J., Measurements of diatom adhesion and their relationship with movement. *Br. Phycol. Bull.*, 3, 2, 195–207, 1967.
[11.27] Hopkins, J. and Drum, R., Diatom motility: An explanation and a problem. *Br. Phycol. Bull.*, 3, 1, 63–67, 1966, URL https://doi.org/10.1080/00071616600650081.
[11.28] Kalbe, L., *Kieselalgen in Binnengewässern: Diatomeen*, VerlagsKG Wolf, Magdeburg, Germany, 2005.
[11.29] Kratochvil, H., email communication (2019/11/28), 2019.
[11.30] Kratochvil, H. and Pollirer, M., Acoustic effects during photosynthesis of aquatic plants enable new research opportunities. *Sci. Rep.*, 7, 44526, 2017.
[11.31] Landau, L. and Lifshitz, E., *Fluid Mechanics*, Second Edition, Volume 6 (Course of Theoretical Physics S), Elsevier, Amsterdam (NL), 1987.
[11.32] Looney, M., An introduction to mems vibration monitoring. *Analog Dialogue*, 48, 06, 1–3, 2014.
[11.33] Purcell, E.M., Life at low Reynolds number. *Am. J. Phys.*, 45, 1, 3–11, 1977, URL https://doi.org/10.1119/ 1.10903.
[11.34] Redfern, P., Mode of isolating naviculae and other test objects. *Q. J. Microsc. Sci.*, 1, 3, 235–236, 1853.
[11.35] Rogers, P. and Trivett, D., *Hydrophone*, AccessScience, (McGraw-Hill Education), New York City, New York, USA, 2014, https://www.accessscience.com/content/hydrophone/330500 (last accessed 2021-01-13.
[11.36] Round, F., Crawford, R., Mann, D., *Diatoms: Biology and Morphology of the Genera*, Cambridge University Press, Cambridge, England, 1990, URL https://books.google. de/books?id=xhLJvNa3hw0C.
[11.37] Sabuncu, A., Gordon, R., Richer, E., Manoylov, K., Beskok, A., The kinematics of explosively jerky diatom motility: A natural example of active nanofluidics, in: *Diatom Gliding Motility [Volume in the series: Diatoms: Biology & Applications, series editors: Richard Gordon & Joseph Seckbach]*, S.A. Cohn, K.M. Manoylov, R. Gordon (Eds.), pp. 33–63, Wiley-Scrivener, Beverly, MA, USA, 2021.
[11.38] SAG, The culture collection of algae at Goettingen university, URL https://www.uni-goettingen.de/en/www.uni-goettingen.de/ de/184982.html (last accessed on 2021/01/14), 2019.
[11.39] Schagerl, M., oral communication (2018/12/11), 2018.
[11.40] Seuss, *Horton Hears a Who!*, Random House, Gütersloh, Germany, 1954.
[11.41] Spiazzi, E. and Mascheroni, R., Mass transfer model for osmotic dehydration of fruits and vegetables—I. Development of the simulation model. *J. Food Eng.*, 34, 4, 387–410, 1997, URL http://www.sciencedirect.com/science/article/ pii/S0260877497001027.
[11.42] Ussing, A., Gordon, R., Ector, L., Buczkó, K., Desnitskiy, A., VanLandingham, S., *The Colonial Diatom "Bacillaria paradoxa": Chaotic Gliding Motility, Lindenmeyer Model of Colonial Morphogenesis, and Bibliography, with Translation of O.F. Müller (1783), "About a*

peculiar being in the beach- water", A.R.G. Ganter Verlag Kommanditgesellschaft, Ruggell, 2005.
[11.43] Utex, Culture collection of algae, https://utex.org (last accessed 2021-01-13), 2019.
[11.44] Wang, J., Cao, S., Du, C., Chen, D., Underwater locomotion strategy by a benthic pennate diatom *Navicula* sp. *Protoplasma*, 250, 1203–1212, 2013.
[11.45] Harper, M.A., Movements, in: *The Biology of Diatoms*, D. Werner (Ed.), pp. 224–249, Blackwell, Oxford, 1977.

Index

Also of Interest

Check out these published and forthcoming related titles from Scrivener Publishing

The Mathematical Biology of Diatoms
Edited by Janice L. Pappas and Richard Gordon
Forthcoming 2022. ISBN 9781119749851

Diatoms Morphogenesis
Edited by Joseph Seckbach and Vadim V. Annenkov
Forthcoming 2021. ISBN 9781119487951

Diatoms Motility
Edited by Stanley A. Cohn, Kalina M. Manoylov and Richard Gordon
Published 2021. ISBN 9781119526353

Diatoms
Fundamentals and Applications
Edited by Joseph Seckbach and Richard Gordon
Published 2019. ISBN 9781119370215

Moving photosynthetic organisms are still a great mystery for biologists and this book summarizes what is known and reports the current understanding and modeling of those complex processes.

The book covers a broad range of work describing our current state of understanding on the topic, including: historic knowledge and misconceptions of motility; evolution of diatom motility; diatom ecology & physiology; cell biology and biochemistry of diatom motility, anatomy of motile diatoms; observations of diatom motile behavior; diatom competitive ability, unique forms of diatom motility as found in the genus *Eunotia;* and models of motility.

This is the first book attempting to gather such information surrounding diatom motility into one volume focusing on this single topic. Readers will be able to gather both the current state of understanding on the potential mechanisms and ecological regulators of motility, as well as possible models and approaches used to help determine how diatoms accomplish such varied behaviors as diurnal movements, accumulation into areas of light, niche partitioning to increase species success. Given the fact that diatoms remain one of the most ecologically crucial cells in aquatic ecosystems, we hope that this volume will act as a springboard towards future research into diatom motility and even better resolution of some of the issues in motility.

Audience

Diatomists, phycologists, aquatic ecologists, cellular physiologists, environmental biologists, biophysicists, diatom nanotechnologists, algal ecologists, taxonomists.

Stanley Cohn is a Professor Emeritus of Biology at DePaul University, Chicago. His lab has been studying ecological conditions affecting diatom cell movement for over 30 years, focusing on the responses to changes in light, temperature, surface, and other ecological factors. He received the Royal Society of Arts Silver Medal and the DePaul University Excellence in Teaching Award.

Kalina Manoylov is professor in Biology at Georgia College and State University and visiting professor at the University of Iowa Lakeside lab. She has a PhD in Zoology and Ecology, Evolutionary Biology and Behavior from Michigan State University. She uses algal-community data to understand environmental changes and anthropogenic effects in different aquatic environments. Her area of expertise is algal and diatom taxonomy and algal ecology. She has published more than 30 peer-reviewed articles, half of them with her students. She is the editor for *PhytoKeys and Frontiers Plant Science*.

Richard Gordon's involvement with diatoms goes back to 1970 with his capillarity model for their gliding motility, published in the *Proceedings of the National Academy of Sciences of the United States of America*. He later worked on a diffusion limited aggregation model for diatom morphogenesis, which led to the first paper ever published on diatom nanotechnology in 1988. He organized the first workshop on diatom nanotech in 2003. His other research is on computed tomography algorithms, HIV/AIDS prevention, and embryogenesis.

Cover design by Russell Richardson
Cover image courtesy of the author

WILEY

www.wiley.com

www.scrivenerpublishing.com

Also available as an e-book

ISBN 978-1-119-52635-3
90000
9 781119 526353